

A Nanosecond Time-Resolved Fluorescence Study of Recombinant Human Myelin Basic Protein

Andrew T. Russo¹ and Ludwig Brand^{1,2}

Received December 21, 1998; accepted March 5, 1999

Myelin basic protein (MBP) is a major component of myelin and plays a central role in the maintenance of its compact multilayered structure. Tryptophan fluorescence is sensitive to environmental factors such as polarity and rotational mobility and often reflects conformational changes in proteins. This work describes a detailed examination of the time-resolved emission properties of the single tryptophan of recombinant human myelin basic protein. Fluorescence decay curves were collected at two separate excitation wavelengths and at different wavelengths across the emission spectrum. The fitting parameters obtained with the aid of global analysis were combined with steady-state emission spectra collected from the same samples and are presented as decay-associated spectra (DAS) and time-resolved emission spectra (TRES). The effects of temperature and binding to anionic membranes on the decay of emission of MBP were investigated. The changes in fitted parameters and the appearance of DAS and TRES as a function of experimental conditions are interpreted in terms of variation in the local environment of the single tryptophan in MBP. The implications of the changes in local environment resulting from experimental treatments are discussed in the context of the overall conformation of MBP and are compared to structural and photophysical properties of MBP obtained from the central nervous system tissue of several species [P. Cavatorta, S. Giovanelli, A. Bobba, P. Riccio, and E. Quagliariello, *Acta Neurol. (Napoli)* **13**, 162–169, (1991); P. Cavatorta, S. Giovanelli, A. Bobba, P. Riccio, A. G. Szabo, and E. Quagliariello, *Biophys. J.* **66**, 1174–1179, 1994; P. Cavatorta, L. Masotti, A. G. Szabo, D. Juretic, P. Riccio, and E. Quagliariello, *Cell Biophys.* **13**, 201–215, 1988].

KEY WORDS: Myelin basic protein; decay-associated spectra; time-resolved emission spectra; global analysis; membrane binding.

INTRODUCTION

Myelin is one of the most abundant membrane structures in the nervous system. Central nervous system (CNS) myelin is formed when oligodendrocytes wrap their cytoplasmic membranes repeatedly around an axon, extruding the cytoplasm to form a compact multilayered membrane sheath. This process is aided by myelin proteins including myelin basic protein (MBP), which is

believed to be very important in stabilization of myelin compaction [1–4]. MBP also has been implicated in different ways in the etiology of multiple sclerosis [5–8].

MBP is localized to a region of myelin called the major dense line, the space between opposed membrane layers on the cytoplasmic face [9,10]. It is believed to bind to the membrane surface by electrostatic interaction with the headgroups of acidic phospholipids and by hydrophobic interaction between nonpolar residues and the lipid acyl chains, although there is no evidence of transmembrane regions [11,12]. MBP may be isolated from CNS myelin [13,14] or produced from an *E. coli* overexpression system where it is purified from inclusion

¹ Department of Biology, The Johns Hopkins University, 3400 North Charles Street, Baltimore, Maryland 21218.

² To whom correspondence should be addressed.

bodies [15]. Protein obtained from traditional sources is water soluble and shows little evidence of ordered structure in solution by various physical methods [16–18]. CNS derived MBP may be separated by cation-exchange chromatography into several charge isomers that are distinguished by the type and number of posttranslational modifications including deamidation and phosphorylation [19]. The isomer most often used in biophysical studies is the most positively charged form and lacks any posttranslational modifications. All of these forms of MBP display lipid vesicle binding activity and aggregate lipid vesicles, especially those containing acidic lipids [20–23]. Some evidence suggests that binding to anionic bilayers induces MBP to adopt a more ordered folded structure than it has free in solution. This more ordered form is characterized by an increase in secondary structure, probably consisting of β -sheet [17,18,24,25].

Recombinant human MBP is immunologically indistinguishable from the most positively charged form of CNS derived MBP but the protein biophysics has not yet been characterized in detail [15]. If adequately characterized it could be a valuable alternative source of MBP for biophysical studies and may be superior to CNS derived MBP for certain types of investigations. The absence of posttranslational modifications and the ease of generating point mutations in these kinds of expression systems are of particular interest. Using the single tryptophan residue present in MBP as a reporter, the steady-state and time-resolved emission properties have been characterized as a function of temperature and binding to vesicles of dimyristoyl phosphatidylglycerol (DMPG). The observed changes in emission properties have been interpreted in terms of changes in solvent environment around tryptophan and possible changes in the protein conformation.

MATERIALS AND METHODS

Solutions

Urea, acetic acid, NaCl, NaOH, HCl, CoCl₂, chloroform, and methanol were purchased from J. T. Baker, Inc., Phillipsburg, NJ. Piperazine-*N*, *N'*-bis[2-ethanesulfonic acid] (PIPES) and phenylmethylsulfonyl fluoride (PMSF) were purchased from Sigma Chemical Co. St. Louis, MO. Ultrapure Tris[hydroxymethyl]aminomethane (Tris) and ultrapure 3-[*N*-morpholino]propanesulfonic acid (MOPS) were obtained from United States Biochemical, Cleveland, OH. Dimyristoyl phosphatidylglycerol (DMPG) was purchased from Avanti polar lipids. All other materials were reagent grade or better.

Myelin basic protein (MBP) was isolated and purified, by a modification of the method of Oettinger and co-workers [15], from *E. coli* BL21(λ DE3), which had been transformed with the pET21a expression vector (Novagen Inc.) carrying the cDNA for the 18.5-kD isoform of human MBP (a generous gift from Dr. Tanya Lewis at Autoimmune Inc.). Briefly, 15 g of frozen induced *E. coli* was thawed and resuspended to a total volume of 30 ml in chilled buffer containing 20 mM MOPS, 150 mM NaCl, 1 mM EDTA, pH 7.4 (SME buffer), with 1 mM PMSF. Cells were broken by two passes through a chilled French pressure cell and inclusion bodies were separated by centrifugation in a Sorval SS-34 rotor spun at 15,000 rpm for 20 min. The insoluble inclusion body pellet was washed once with 40 ml SME. The wash supernatant was discarded and the resulting pellet was dissolved in 20 mM MOPS, 8 M urea, 1 mM PMSF, 1 mM EDTA, pH 7.2 (solubilization buffer), by gentle pipeting. Urea-solubilized inclusion bodies were spun in the SS-34 rotor at 15,000 rpm for 30 min to remove urea-insoluble material and the resulting supernatant was applied in batch to a 15-ml SP-sepharose FF cation-exchange resin (Pharmacia) preequilibrated in the solubilization buffer. The Sepharose was then packed in a 2.5-cm Bio-Rad econo column and washed until the OD₂₈₀ was less than 0.05. Elution of MBP was accomplished by the application of solubilization buffer containing 300 mM NaCl. Eluate was monitored by absorbance at 280 nm and material was collected in 5-ml aliquots until the OD₂₈₀ of the eluted material was less than 0.05. This material was pooled and diluted two fold with 20 mM MOPS, 4 M urea, pH 7.2 (Buffer A). This material was then passed through a 0.22- μ m filter (Millipore) and the filtrate applied to a Pharmacia Mono-S HR-10/10 cation-exchange column equilibrated in a mixture of 85% buffer A and 15% 20 mM MOPS, 4 M urea, 1 M NaCl (buffer B) using a Pharmacia FPLC system. Bound material was eluted at a flow rate of 0.5 ml min⁻¹ by a gradient of 150–400 mM NaCl (15–40% buffer B). The column run was monitored by absorbance at 280 nm and all eluted fractions were analyzed by SDS-PAGE. Pooled fractions containing MBP were then applied to a 5-ml Pharmacia HiLoad chelating column loaded with Co²⁺ equilibrated in 25 mM PIPES, 25 mM sodium acetate (NaOAc), 500 mM NaCl, pH 7.0 (IMAC buffer A), using the Pharmacia FPLC system. The column was then washed with 40% 25 mM PIPES, 25 mM NaOAc, 500 mM NaCl, pH 4.5 (IMAC buffer B), until OD₂₈₀ showed a stable baseline. MBP was eluted at 2 ml min⁻¹ with a 300-ml pH gradient from 40 to 100% IMAC buffer B. Purity of material was determined by Coomassie-stained SDS-PAGE and fractions of greater than 98%

purity were saved and stored at -20°C until used without further purification.

Concentration of samples was determined spectrophotometrically using $E_{276.4}^{1\text{mg/ml}} = 0.564$, determined for the homologous bovine MBP [26]. Absorbance measurements were made on a Shimadzu UV160U UV/vis spectrophotometer. Steady-state spectra were obtained on an SLM 48000 spectrofluorometer. The cell holder was maintained at the indicated temperatures using a circulating water bath. Time-resolved measurements were made using the time-correlated single-photon counting method on a picosecond synchronously pumped, mode-locked dye laser system (Spectra Physics 3000 series) as described previously [27]. Data were collected at 13 ps per channel in 2048 channels. Decay of fluorescence intensity was described as a sum of exponentials according to

$$I(t) = \sum \alpha_i e^{-t/\tau_i} \quad (1)$$

where τ_i is the lifetime of component i of the emission decay and α_i is its associated preexponential factor. Single decay curves were analyzed by a nonlinear least-squares curve-fitting procedure [28] using the program TCPHOTON. Global analysis [29] with τ_i linked over all emission wavelengths was performed with LGLOBALS (written by Dmitri Topygin). The resulting fitting parameters in combination with steady-state spectra were then used to generate decay-associated spectra (DAS) and time-resolved emission spectra (TRES) [30,31].

Large unilamellar vesicles (100 nm) were prepared in a Lipex Extruder (Lipex Biomembranes Inc.). DMPG dissolved in chloroform/methanol was dried in a shell in a 13×100 -mm disposable glass tube under a stream of dry nitrogen and hydrated in the appropriate volume of buffer (20 mM MOPS, pH 7.2). Prior to extrusion, any additional material (i.e., MBP) was added to the multilamellar suspension, which was then adjusted to 4-ml total volume and passed through five freeze-thaw cycles using a dry ice-ethanol bath and a 40°C water bath. After the final thaw the suspension was passed 10 times under pressure through two stacked $0.1\text{-}\mu\text{m}$ polycarbonate filters and used within 12 h.

RESULTS

The fluorescence decay of MBP as a function of emission wavelength was collected under conditions of varying excitation wavelength, temperature, and in the presence and absence of DMPG vesicles. The majority of decays were best described as a sum of four exponential

Table I. Global Fitting Parameters for Decays of $15\ \mu\text{M}$ MBP in 20 mM MOPS at pH 7.2

Sample	τ_1	τ_2	τ_3	τ_4	χ^2
30°C					
289 nm	0.27	1.02	2.34	4.47	1.005
295 nm	0.25	0.94	2.35	4.64	1.002
10°C					
289 nm	0.32	1.30	3.36	5.68	0.995
295 nm	0.27	1.14	3.27	5.90	0.995
30°C, + DMPG					
289 nm	0.31	1.35	3.68	9.55	1.007
295 nm	0.36	1.44	3.87	10.90	1.033

components except those collected on the red edge of the spectrum, which required only three components for an adequate fit. Since lifetime values did not fluctuate significantly as a function of emission wavelength, all decay curves for each set of experimental conditions were reanalyzed using global analysis. The lifetimes and global χ^2 values resulting from the fits are presented in Table I. Using 30°C as the reference, both a temperature decrease to 10°C and the addition of DMPG vesicles cause an increase in all lifetime components. The relative increases are presented in Table II. In the case of decreasing temperature, the lifetimes show moderate increases, with the largest change in the second longest lifetime (τ_3). The increases in lifetimes upon binding to DMPG vesicles are large and are dominated by the increase in the longest lifetime (τ_4), which is more than doubled.

The global parameters in Table I and associated local preexponential factor were combined with the steady-state spectra for each data set and used to generate DAS (Figs. 1–3) and TRES (Figs. 4–6). From these plots it can be seen that excitation wavelength has minimal effects on the emission decay properties of MBP except at the blue edge of emission, where a shoulder appears at short times after excitation. These effects are not visible in samples

Table II. Relative Increases in Lifetimes Resulting from a Decrease in Temperature and Binding to DMPG Vesicles

	Ratio			
	τ_1	τ_2	τ_3	τ_4
10°C/30°C				
289	1.19	1.27	1.44	1.27
295	1.08	1.21	1.39	1.27
DMPG/30°C				
289	1.15	1.32	1.57	2.14
295	1.44	1.53	1.65	2.35

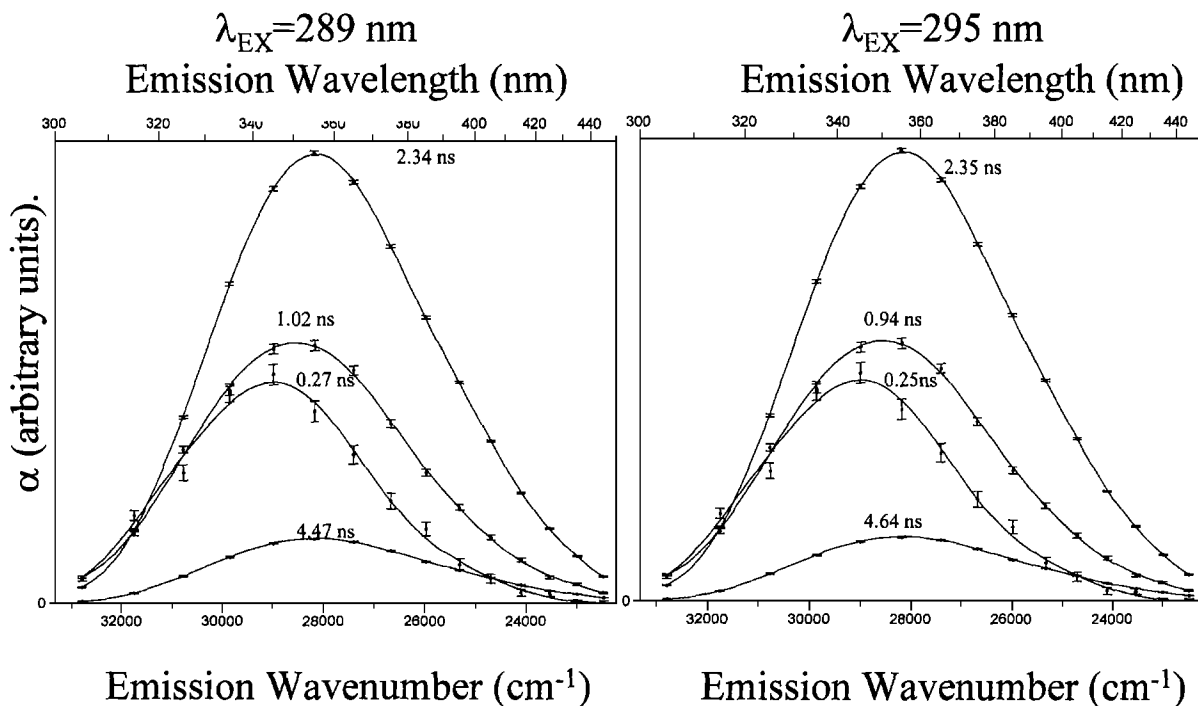


Fig. 1. DAS for 15 μM MBP in 20 mM MOPS, pH 7.2, at 30°C excited at 289 or 295 nm.

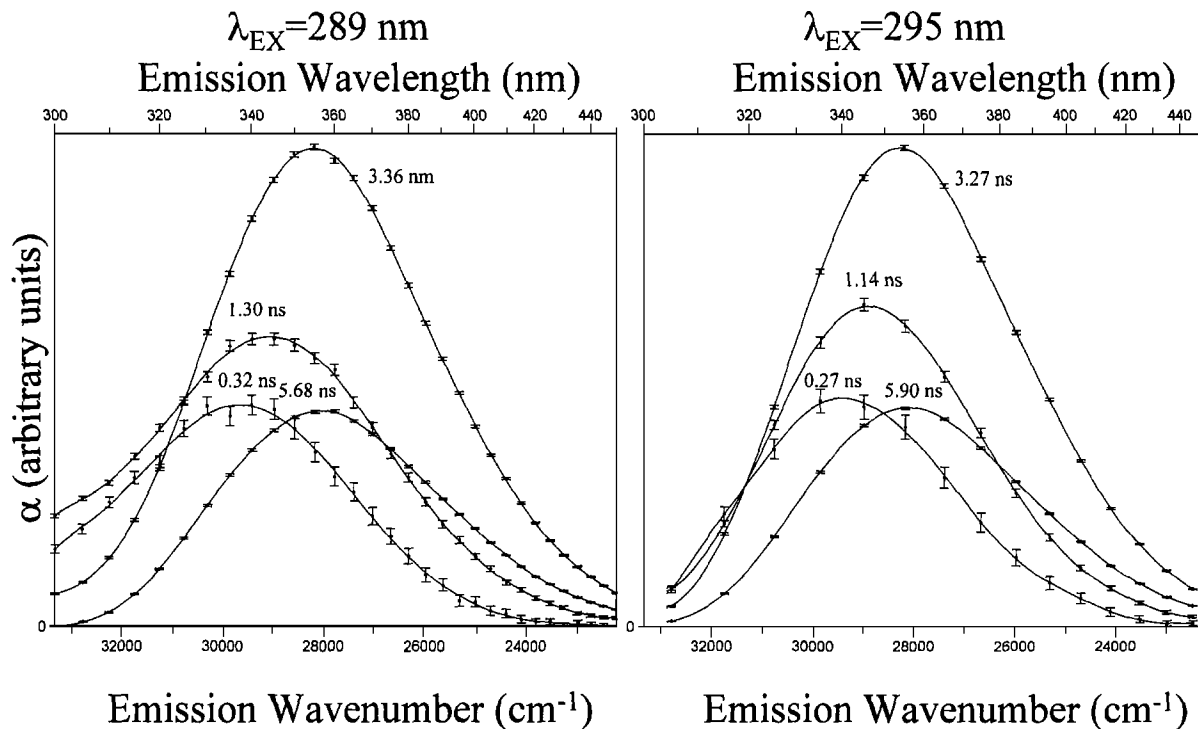


Fig. 2. DAS for 15 μM MBP in 20 mM MOPS, pH 7.2, at 10°C excited at 289 or 295 nm.

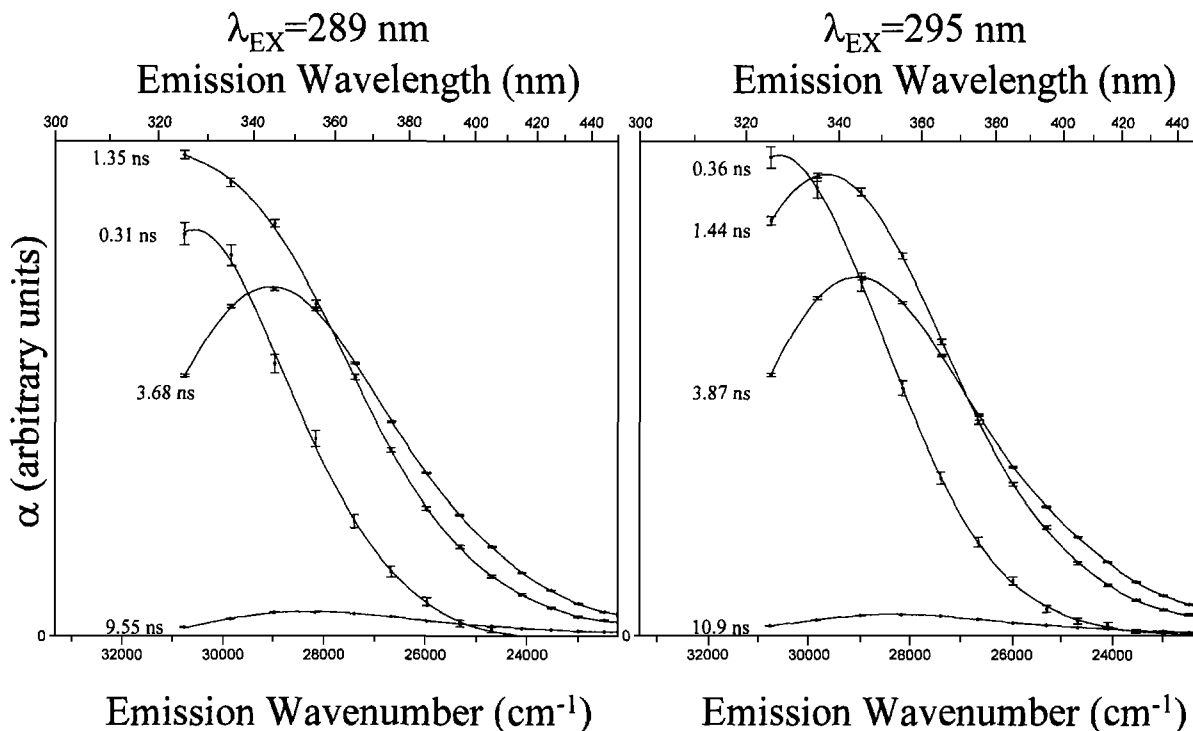


Fig. 3. DAS for 10 μ M MBP in 20 mM MOPS, pH 7.2, at 30°C in the presence of 100-nm DMPG LUVs (140 μ g/ml phospholipid) excited at 289 or 295 nm.

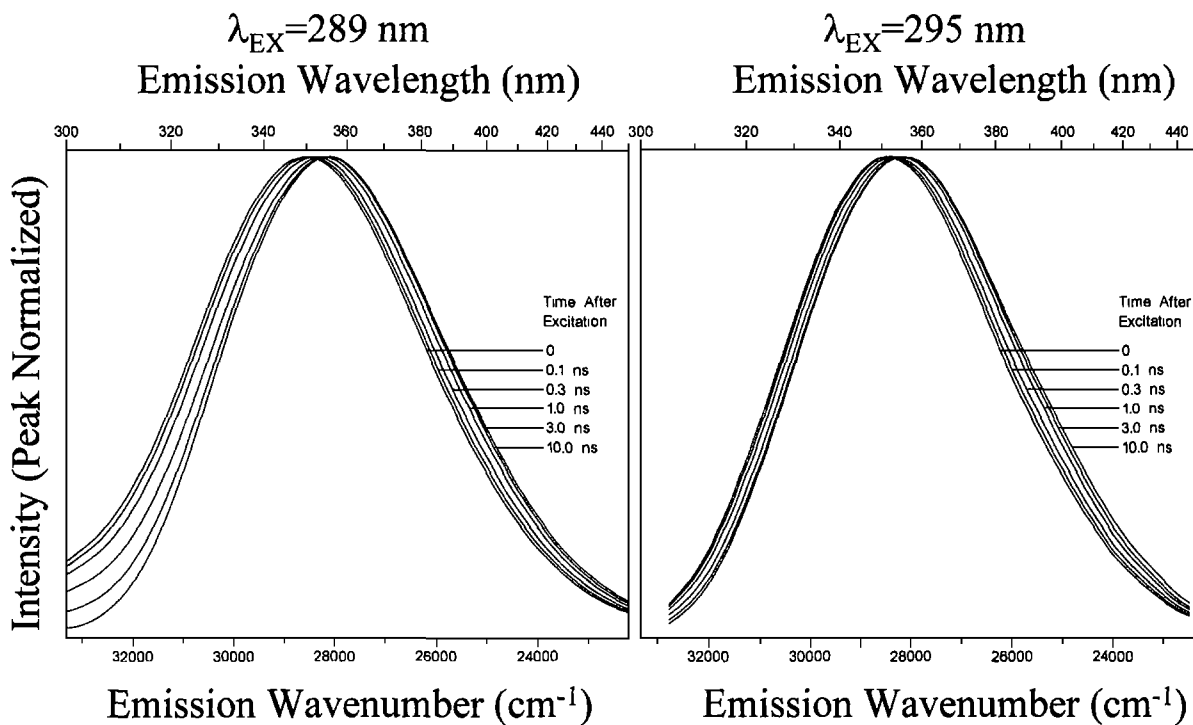


Fig. 4. TRES for 15 μ M MBP in 20 mM MOPS, pH 7.2, at 30°C excited at 289 or 295 nm.

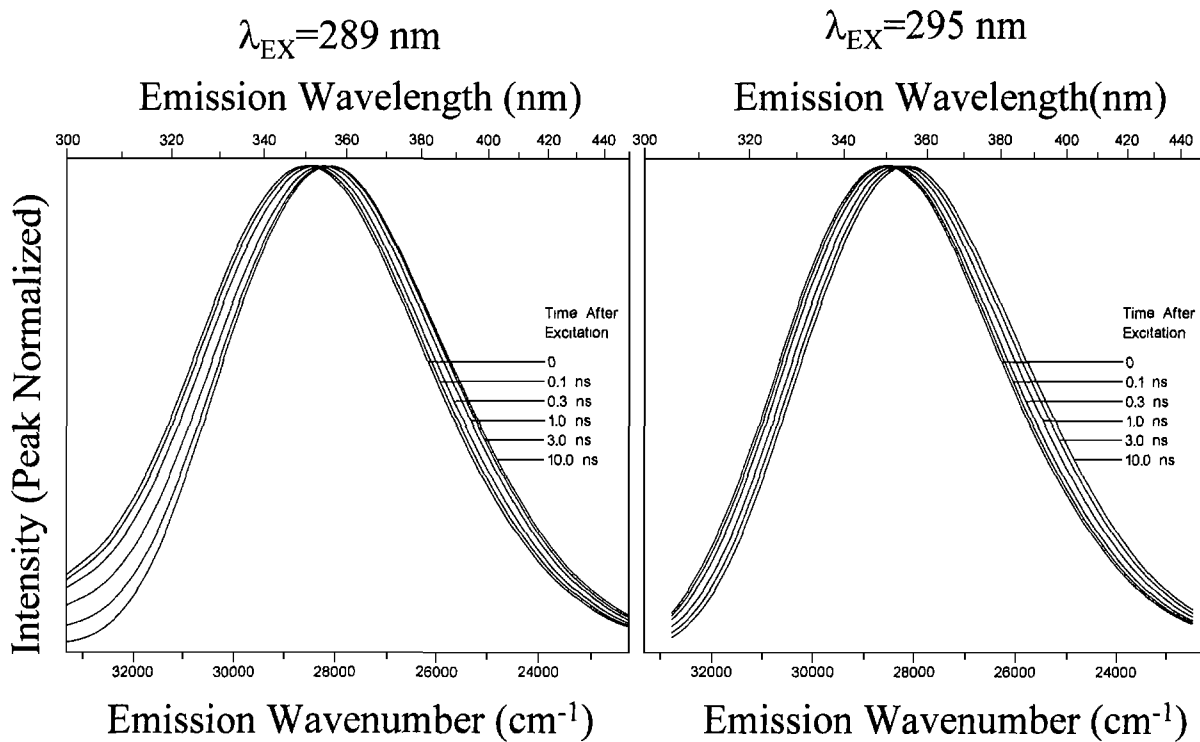


Fig. 5. TRES for 15 μM MBP in 20 mM MOPS, pH 7.2, at 10°C excited at 289 or 295 nm.

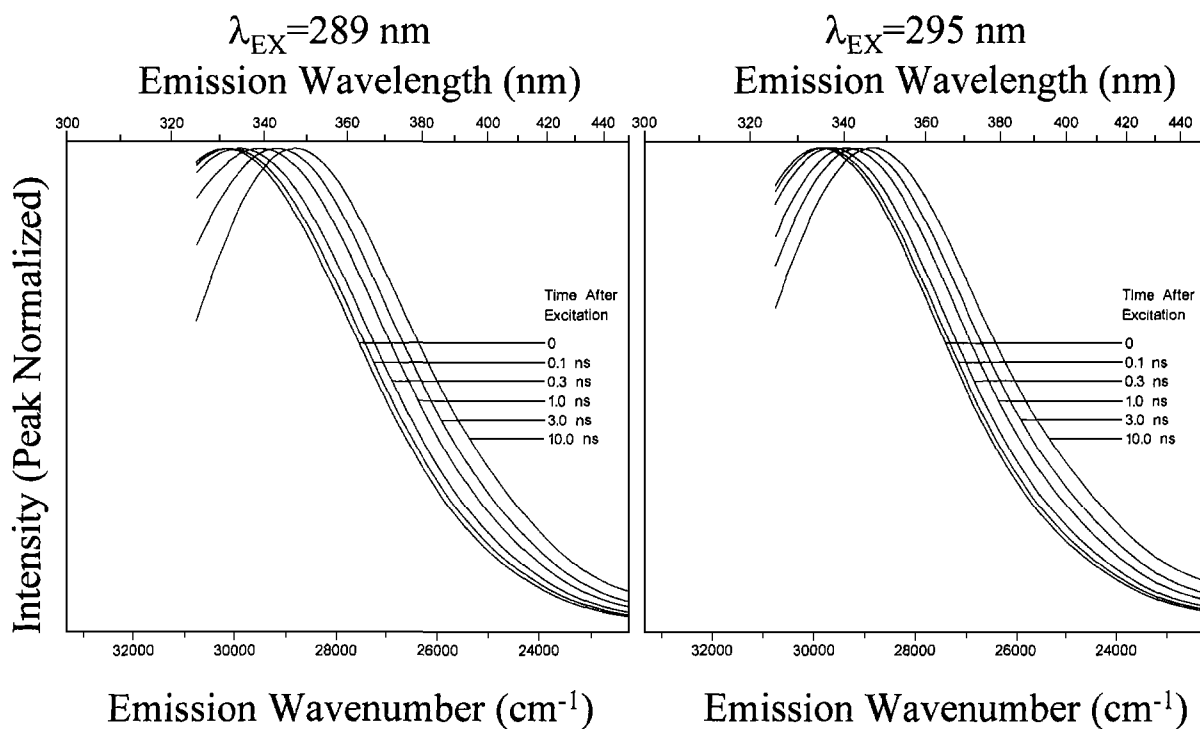


Fig. 6. TRES for 10 μM MBP in 20 mM MOPS, pH 7.2 at 30°C with 100-nm DMPG LUVs (140 $\mu\text{g}/\text{ml}$ phospholipid) excited at 289 or 295 nm.

containing DMPG since it was necessary to eliminate shorter-wavelength data during analysis due to light-scattering artifacts introduced by the vesicle suspensions.

Figure 1 shows the DAS for MBP in 20 mM MOPS buffer at pH 7.2 and 30°C. These are the reference conditions to which all other experiments in this study are compared. Under these conditions the 2.35-ns lifetime has the largest preexponential factor (α) throughout most of the emission spectrum. The spectrum associated with the 4.64-ns lifetime exhibits the smallest α over most of the wavelength range except at the red edge. The α 's associated with the 0.25- and 0.94-ns lifetimes are similar at the blue end of the spectrum but diverge toward the red, with the 0.94-ns component being slightly higher.

Ground-state heterogeneity and excited-state processes may both contribute to multiexponential decay kinetics in single tryptophan proteins. To characterize the contribution of these two conditions on the fluorescence properties of the single tryptophan of MBP, fluorescence decays were collected as above except at a temperature of 10°C. The DAS from this experiment are shown in Fig. 2. Immediately apparent, compared to the previous DAS, is the increase in the relative contribution from the longest lifetime (5.90 ns) at all wavelengths measured. The decay-associated spectra for the other three lifetimes (3.27, 1.14, and 0.27 ns) are similar to those obtained at 30°C.

Several studies have shown that upon binding to anionic membranes MBP adopts a more ordered structure than that observed in buffered solution [11,17,18,25,32]. It was of interest to us to see whether this increase in ordered structure would be reflected in the time-resolved emission properties of MBP. Decay data were collected as in the first experiment but with the addition of anionic DMPG vesicles. The effects on the DAS are shown in Fig. 3. The DAS of MBP in the presence of membranes shows substantial differences from DAS in buffer alone. All spectra are blue shifted in the presence of membranes and a marked increase in the values of α for the two shorter lifetimes (0.36 and 1.44 ns) is observed at the majority of emission wavelengths. In contrast, the contributions of the longer lifetimes (10.9 and 3.87 ns) relative to one another are not affected.

Figures 4 to 6 show the TRES that correspond to the DAS in Figs. 1 to 3, respectively. The red shift of these spectra as a function of time is summarized in Fig. 7, where the emission frequency determined at the half-height position of the red edge of each spectrum is plotted versus time. The spectra under all experimental conditions shift to the red with time. In the absence of DMPG there seems to be little effect of excitation wavelength on the characteristics of this shift as indicated by the

almost-negligible separation between the curves obtained with two excitation wavelengths. The movement of the curves is of the order of 400 cm^{-1} and is essentially completed by 10 ns after excitation. In the presence of DMPG the emission is blue shifted and the position of the TRES at 0 ns after excitation varies with excitation wavelength, excitation at 289 giving a blue shift of 130 cm^{-1} relative to that observed with 295-nm excitation. By about 1 ns postexcitation the positions of the spectra from excitation at 289 and 295 converge and continue to shift toward the red, covering a total distance of over 1100 cm^{-1} , with no indication of completion by 10 ns.

DISCUSSION

There is much disagreement about the origin of non-exponential decay kinetics of tryptophan emission in proteins. The different physical phenomena that may account for this behavior include various excited state processes such as solvent and side-chain relaxation [33–38], processes that contribute to the rate of nonradiative decay to the ground state [39] and structural effects that may influence the other processes [35, 40–44]. A better understanding of the factors influencing the spectroscopic properties of tryptophan will allow a more detailed description of the environment around the single tryptophan in MBP, which can be used to monitor more general conformational changes resulting from careful manipulation of the proteins environment.

Recombinant human MBP in aqueous buffer at pH 7.2 showed an emission spectrum characteristic of a highly solvent exposed tryptophan which is in agreement with previously published results obtained using homologous MBPs from the CNS tissue of several other species [26,32,45–47]. Time-resolved decays of emission were similar to those reported previously for bovine MBP [26,48] except that an additional exponential decay component was required to achieve an adequate fit in the global analysis of decays collected at multiple emission wavelengths. Single-curve analysis through most of the emission spectrum required four exponential components for an adequate fit to the data except at the far red edge, where the decays required only three components to fit. This may be due to the reduced number of counts collected at the red edge since each decay was collected for an equal period of time or the reduced preexponential of the shortest decay component, which is nearly zero at these wavelengths in the global analysis. In this case the longest and shortest lifetimes were comparable between recombinant human MBP and bovine MBP, while the middle lifetime from a three-component fit was split into

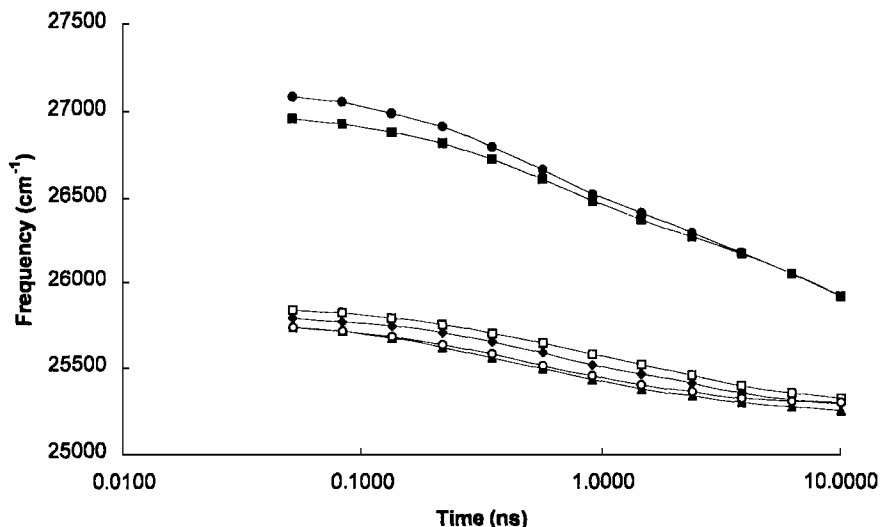


Fig. 7. Position of the red edge at the half-height of TRES of MBP under all conditions tested as a function of time after excitation. Excitation at 295 nm, and (○) 30°C, (□) 10°C, and (■) 30°C with DMPG vesicles. Excitation at 289 nm, and (▲) 30°C, (◆) 10°C, and (●) 30°C with DMPG vesicles.

a shorter and longer lifetime when fitting a four-component model.

Variation of excitation wavelength has little effect on the emission decay parameters of MBP in solution at either 10 or 30°C (Table I). The most obvious effect of varying the excitation wavelength was in the shape of the DAS and TRES. At 289-nm excitation there is a shoulder on the blue edge of the spectra for short-lifetime components in the DAS and at short times in the TRES. This is absent when excitation is at 295 nm. It is likely that this shoulder is due to contributions from tyrosine since it is seen at both blue-shifted excitation and emission and occurs at short times in the decay. The steady-state emission spectrum of MBP is very red shifted, which is indicative of a polar environment around the tryptophan. The TRES also starts very far to the red and continues to move even farther to the red with time, almost completing its movement during the lifetime of the excited state as shown in Figs. 4, 5, and 7. This indicates that the processes contributing to the change in environment occur during the excited-state lifetime of the tryptophan. An alternative explanation involves the presence of multiple species that cannot interconvert on the nanosecond time scale and have absorption and emission properties different from one another. The former model is dynamic in nature and suggests that we can obtain information about the rate of relaxation processes in the environment of the tryptophan, while the latter situation is static and gives a snapshot of equilibrium populations of the different ground state species present. These two explanations are not necessarily exclusive.

MBP is believed to exist in a predominantly unfolded state in solution with no defined compact structure [16,49]. However, it has been postulated that small regions of structure may be present in aqueous MBP and these include the region containing the single tryptophan [11,50]. Structure in the local environment around the tryptophan of MBP could explain the red shift of the TRES that we observe. The steady-state emission spectrum of MBP is characteristic of solvent-exposed tryptophan and is very much like that of aqueous NATA, however, in the case of complete solvent exposure, no red shift of the emission spectrum over time is expected. The red shift of the TRES over time argues strongly that either the local environment around the tryptophan is motionally restricted or that there are multiple ground-state conformations.

Figure 7 shows the position of the red edge of the TRES determined at one-half the maximum height as a function of time after excitation for all conditions. At the chosen reference conditions there is a small frequency shift in TRES over time studied (lower curves, triangles and open circles). The effect of excitation wavelength on the properties of the TRES is negligible. Under these conditions, processes contributing to the time-dependent red shift, excited-state solvent relaxation, or ground-state heterogeneity cannot be distinguished.

Binding to anionic liposomes results in dramatic changes in the fluorescence properties of MBP. The blue shift in the steady-state emission spectrum indicates decreased solvent exposure of the tryptophan. This is consistent with a stabilization of defined structure in MBP

upon binding to negatively charged membranes and is in agreement with previous studies on CNS derived MBP [11,25,51,52]. When MBP folds in this way the single tryptophan may become buried in a hydrophobic core or positioned at an interface in MBP multimers. Regions of the MBP chain may also extend down past the lipid headgroups and interact directly with the lipid acyl chains [12,17,48,53–56]. Any of these possibilities could account for the blue shift and the observed increase in the lifetimes. In the presence of vesicles there is a large increase in the α 's for the two shortest lifetimes relative to the longer lifetimes as shown in the DAS in Fig. 3. The positions of the TRES (Fig. 7; filled squares and circles) obtained at different excitation wavelengths are initially separated and converge after about 1 ns. The total red shift is threefold greater than for MBP in buffer alone (lower curves) and shows no indication of an end point after 10 ns. As in the case of MBP in buffer alone, these observations are insufficient to distinguish the existence of multiple ground-state conformations or excited-state dipole relaxation.

Aqueous recombinant human MBP in solution is indistinguishable from the C1 fraction of CNS derived MBP by the methods of steady-state emission and time-resolved decay of emission. Additionally, recombinant MBP binds to anionic lipid vesicles with concomitant changes in its photophysical properties consistent with reduced exposure of the single tryptophan to solvent and an increase in ordered structure in agreement with earlier work on homologous MBPs. We believe that the availability and ease of production of recombinant MBP from a standard overexpression system will greatly facilitate further studies of this protein. In particular, the ability to produce site-specific mutations will allow us to address more specific questions regarding the structure of the membrane-associated form of the protein and its function in the maintenance of myelin structure.

ACKNOWLEDGMENTS

We thank Dr. Tanya Lewis for the gift of MBP cDNA, Dr. Dmitri Topygin for help in operation of the time-correlated single-photon counting instrument as well as analysis and interpretation of the data, and Vikas Nanda and Dr. Michael Rodgers for helpful discussions and suggestions. This work was supported by NSF Grant MCB-98/0812.

REFERENCES

1. R. Martini and M. Schachner (1997) *Glia* **19**, 298–310.
2. H. Inouye and D. A. Kirschner (1988) *Biophys. J.* **53**, 247–260.
3. H. Inouye and D. A. Kirschner (1988) *Biophys. J.* **53**, 235–245.
4. R. P. Rand, N. L. Fuller, and L. J. Lis (1979) *Nature* **279**, 258–260.
5. S. Sriram and M. Rodriguez (1997) *Neurology* **48**, 464–470.
6. P. Stinissen, J. Raus, and J. Zhang (1997) *Crit. Rev. Immunol.* **17**, 33–75.
7. C. M. Deber, D. W. Hughes, P. E. Fraser, A. B. Pawagi, and M. A. Moscarello (1986) *Arch. Biochem. Biophys.* **245**, 455–463.
8. M. A. Moscarello, G. W. Brady, D. B. Fein, D. D. Wood, and T. F. Cruz (1986) *J. Neurosci. Res.* **15**, 87–99.
9. E. Barbarese, C. Barry, C. H. Chou, D. J. Goldstein, G. A. Nakos, R. Hyde-DeRuyscher, K. Scheld, and J. H. Carson (1988) *J. Neurochem.* **51**, 1737–1745.
10. F. X. Omlin, H. D. Webster, C. G. Palkovits, and S. R. Cohen (1982) *J. Cell Biol.* **95**, 242–248.
11. R. Smith (1992) *J. Neurochem.* **59**, 1589–1608.
12. M. B. Sankaram, P. J. Brophy, and D. Marsh (1989) *Biochemistry* **28**, 9685–9691.
13. R. E. Martenson, G. E. Deibler, and M. W. Kies (1969) *J. Biol. Chem.* **244**, 4268–4272.
14. G. E. Deibler, R. E. Martenson, and M. W. Kies (1972) *Prep. Biochem.* **2**, 139–165.
15. H. F. Oettinger, A. Al-Sabbagh, Z. Jingwu, J. M. LaSalle, H. L. Weiner, and D. A. Hafler (1993) *J. Neuroimmunol.* **44**, 157–162.
16. A. Gow and R. Smith (1989) *Biochem. J.* **257**, 535–540.
17. W. K. Surewicz, M. A. Moscarello, and H. H. Mantsch (1987) *Biochemistry* **26**, 3881–3886.
18. M. A. Keniry and R. Smith (1979) *Biochim. Biophys. Acta* **578**, 381–391.
19. R. Zand, M. X. Li, X. Jin, and D. Lubman (1998) *Biochemistry* **37**, 2441–2449.
20. J. M. Boggs, P. M. Yip, G. Rangaraj, and E. Jo (1997) *Biochemistry* **36**, 5065–5071.
21. E. Jo and J. M. Boggs (1995) *Biochemistry* **34**, 13705–13716.
22. T. Pali, B. Ebert, and L. I. Horvath (1987) *Biochim. Biophys. Acta* **904**, 346–352.
23. A. J. Steck, H. P. Siegrist, P. Zahler, and N. N. Herschkowitz (1976) *Biochim. Biophys. Acta* **455**, 343–352.
24. C. S. Randall and R. Zand (1985) *Biochemistry* **24**, 1998–2004.
25. B. H. Stuart (1996) *Biochem. Mol. Biol. Int.* **38**, 839–845.
26. P. Cavatorta, S. Giovanelli, A. Bobba, P. Riccio, A. G. Szabo, and E. Quagliariello (1994) *Biophys. J.* **66**, 1174–1179.
27. P. G. Wu, K. G. Rice, L. Brand, and Y. C. Lee (1991) *Proc. Natl. Acad. Sci. USA* **88**, 9355–9359.
28. A. Grinvald and I. Z. Steinberg (1974) *Anal. Biochem.* **59**, 583–598.
29. J. M. Beechem, E. Gratton, M. Ameloot, J. R. Knutson, and L. Brand, in J. R. Lakowicz (Ed.), *Topics in Fluorescence Spectroscopy: Principles, Vol. 2*, Plenum Press, New York and London, p. 241.
30. J. H. Easter, R. P. DeToma, and L. Brand (1976) *Biophys. J.* **16**, 571–583.
31. W. R. Ware, S. K. Lee, G. J. Brant, and P. P. Chow (1971) *J. Chem. Phys.* **54**, 4729.
32. C. Nicot, M. Vacher, M. Vincent, J. Gallay, and M. Waks (1985) *Biochemistry* **24**, 7024–7032.
33. A. P. Demchenko and A. S. Ladokhin (1988) *Eur. Biophys. J.* **15**, 369–379.
34. P. R. Callis and B. K. Burgess (1997) *J. Phys. Chem. B* **101**, 9429–9432.
35. B. Hudson (1999) *Acc. Chem. Res.* **32**, 297–300.
36. J. R. Lakowicz and A. Balter (1982) *Photochem. Photobiol.* **36**, 125–132.
37. J. R. Lakowicz and H. Cherek (1980) *J. Biol. Chem.* **255**, 831–834.
38. A. Chattopadhyay and R. Rukmini (1993) *FEBS Lett.* **335**, 341–344.
39. Y. Chen and M. D. Barkley (1998) *Biochemistry* **37**, 9976–9982.
40. R. F. Chen, J. R. Knutson, H. Ziffer, and D. Porter (1991) *Biochemistry* **30**, 5184–5195.
41. C. Royer (1993) *Biophys. J.* **65**, 9–10.

42. A. G. Szabo and D. M. Rayner (1980) *J. Am. Chem. Soc.* **102**, 554–563.
43. J. W. Petrich, M. C. Chang, D. B. McDonald, and G. R. Fleming (1983) *J. Am. Chem. Soc.* **105**, 3824–3832.
44. N. D. J. Silva and F. G. Prendergast (1996) *Biophys. J.* **70**, 1122–1137.
45. A. J. Jones and M. G. Rumsby (1975) *J. Neurochem.* **25**, 565–572.
46. S. J. Morris, D. Bradley, A. T. Campagnoni, and G. L. Stoner (1987) *Biochemistry* **26**, 2175–2182.
47. M. W. Nowak and H. A. Berman (1991) *Biochemistry* **30**, 7642–7651.
48. P. Cavatorta, L. Masotti, A. G. Szabo, D. Juretic, P. Riccio, and E. Quagliariello (1988) *Cell Biophys.* **13**, 201–215.
49. J. Sedzik and D. A. Kirschner (1992) *Neurochem. Res.* **17**, 157–166.
50. E. C. J. Alvord, S. Hruby, R. E. Martenson, G. E. Deibler, and M. J. Law (1986) *J. Neurochem.* **47**, 764–771.
51. R. A. Ridsdale, D. R. Beniac, T. A. Tompkins, M. A. Moscarello, and G. Harauz (1997) *J. Biol. Chem.* **272**, 4269–4275.
52. C. Nicot, M. Vacher, L. Denoroy, P. C. Kahn, and M. Waks (1993) *J. Neurochem.* **60**, 1283–1291.
53. M. Roux, F. A. Nezil, M. Monck, and M. Bloom (1994) *Biochemistry* **33**, 307–311.
54. P. E. Fraser, R. P. Rand, and C. M. Deber (1989) *Biochim. Biophys. Acta* **983**, 23–29.
55. J. M. Boggs, L. S. Chia, G. Rangaraj, and M. A. Moscarello (1986) *Chem. Phys. Lipids* **39**, 165–184.
56. G. L. Mendz, W. J. Moore, L. R. Brown, and R. E. Martenson (1984) *Biochemistry* **23**, 6041–6046.